

Effect of Fiber Concentration and Axial Ratio on the Rheological Properties of Cellulose Fiber Suspensions

Daisuke TATSUMI, Satoshi ISHIOKA, and Takayoshi MATSUMOTO*

*Division of Forest and Biomaterials Science, Graduate School of Agriculture,
Kyoto University, Kyoto 606-8502, Japan*

(Received: September 28, 2001)

The steady flow and the dynamic viscoelastic properties of cellulose fiber suspensions were investigated as functions of the suspension concentration and the fiber shape using a parallel-plate type rheometer. Various concentrations of the suspensions were made from various types of cellulose fibers, i.e., microcrystalline cellulose, bacterial cellulose, and fibrillated cellulose fibers. All the suspensions showed non-Newtonian flow even at very low concentrations. The flow property of each suspension showed a plateau of the shear stress, i.e., the yield stress, over a critical concentration. The critical concentration obtained from the experiment agreed well with the value theoretically calculated from the axial ratio of the fibers. The dynamic moduli of the suspensions were almost independent of the angular frequency, and they increased with the fiber concentration. The dynamic storage moduli increased in proportion to the 9/4th power of the fiber concentration. This power of 9/4 is coincident with that theoretically required for polymer gels. This fact suggests that the rigidity of the suspensions has appeared by the same mechanism from the order of cellulose fibers to microcrystalline cellulose fibers, and even to polymer molecules.

Key Words: Cellulose fibers / Suspensions / Axial ratio / Rheology / Power law

1. INTRODUCTION

Fiber suspensions generally have remarkably higher viscosity and elasticity than spherical particle suspensions of equal volume concentration. It makes them hard to deal with in various industrial fields. For example, in the paper industry, the viscosity of the pulp fiber suspension is controlled by maintaining very low fiber concentration around 1% in order to make the suspension flow uniformly. However, such a low concentration is disadvantageous for energy and water consumption. Therefore, further efficiency improvement has been required to control such characteristics of the fiber suspensions.

Many researchers have made efforts to clarify the characteristics of the fiber suspensions. Mason¹⁾ paid attention to the large excluded volume of a fiber. He proposed the following equation for the critical concentration, c_0 , at which fibers are no longer able to undergo free rotation:

$$c_0 = V_a/V_e = 3/(2p^2) \quad (1)$$

where V_a is the actual volume of a fiber, V_e is the effective volume swept out by a rotating fiber and is equal to that of a sphere whose diameter equals the fiber length, and p is the

axial ratio (length/diameter) of the fiber. When the concentration of a suspension is over c_0 , the effect of the fiber network structure due to the fiber-fiber interaction becomes important. Some researchers have measured the fiber network strength using simple tensile tests for solidified cellulose suspensions.^{2,3)} Kerekes *et al.*⁴⁾ summarized these experimental results in a simple power equation:

$$\sigma_y = kc_m^\alpha \quad (2)$$

where σ_y is the yield stress of the suspension, c_m is the mass concentration of the suspension, and k and α are constants. They have reported that the constants are unique for every suspension and the values are in the intervals of $1.18 < k < 24.5$ and $1.26 < \alpha < 3.02$, respectively. Bennington *et al.*⁵⁾ have extended the equation theoretically:

$$\sigma_y = k'Ep^2c_v^3 \quad (3)$$

where c_v is the volumetric concentration of the suspension and E is Young's modulus of the fiber. However, they found that this equation does not agree with their experimental results as to the powers of E and p .

Recently, many researchers have measured the fiber network strength using disruptive shear tests.⁶⁻⁸⁾ However,

there have been few investigations that deal with a rotational rheometer systematically. In a previous study,⁹⁾ we investigated the effect of the fiber concentrations on the rheological properties of the cellulose fiber suspensions. In the present study, we investigated the effect of not only the fiber concentrations but also the axial ratio of the fiber on the rheological properties of the suspensions. We also examined what the constants k and α depend on. The relationships between the moduli of the suspension and the fiber concentration were observed and discussed.

2. EXPERIMENTAL

2.1 Materials

One of the cellulose fibers used in this study was made in our laboratory by hydrolysis of the cotton cellulose Whatman® CF11. It was prepared by treating 10 g of CF11 with 200 ml of 4N hydrochloric acid at 80°C for 225 min.¹⁰⁾ It was repeatedly washed with centrifugation and then dialyzed with distilled water until the electrical conductivity of the outer liquid became equal to that of distilled water. This takes almost a month. An ultrasonic treatment is required to refine the

hydrolyzed CF11. The treatment was done with an ultrasonic disrupter (UD-200, Tomy Seiko Co., Ltd., Japan) for 1 hour at a frequency of 20 kHz, and the microcrystalline cellulose fiber obtained was named CF11H. Another fiber sample was a commercial product Ceolus® FP-3, kindly supplied by Asahi Kasei Corporation, Japan. Bacterial cellulose (BC) used in this study was kindly supplied by Bio-Polymer Research Co., Ltd., Japan. A part of it was hydrolyzed, centrifuged, and purified by dialysis as described above, and it was called BCH. Celish® KY-100G microfibrillated cellulose made from purified wood pulp, kindly supplied by Dical Chemical Industries, Ltd., Japan, was also used. Before measurements, all the cellulose fibers were dispersed in distilled water to a required concentration and then treated by the ultrasonic disrupter for 5 min in order to disperse them thoroughly.

The cellulose fibers were observed with a scanning electron microscope (SEM: JSM-T330A, JEOL, Ltd., Japan) or an atomic force microscope (AFM: NV2000, Olympus Optical Co., Ltd., Japan), as shown in Fig. 1. The average lengths L and diameters D of the fibers are shown in Table I with the calculated axial ratios p . The diameter of BC was not changed by the hydrolysis.

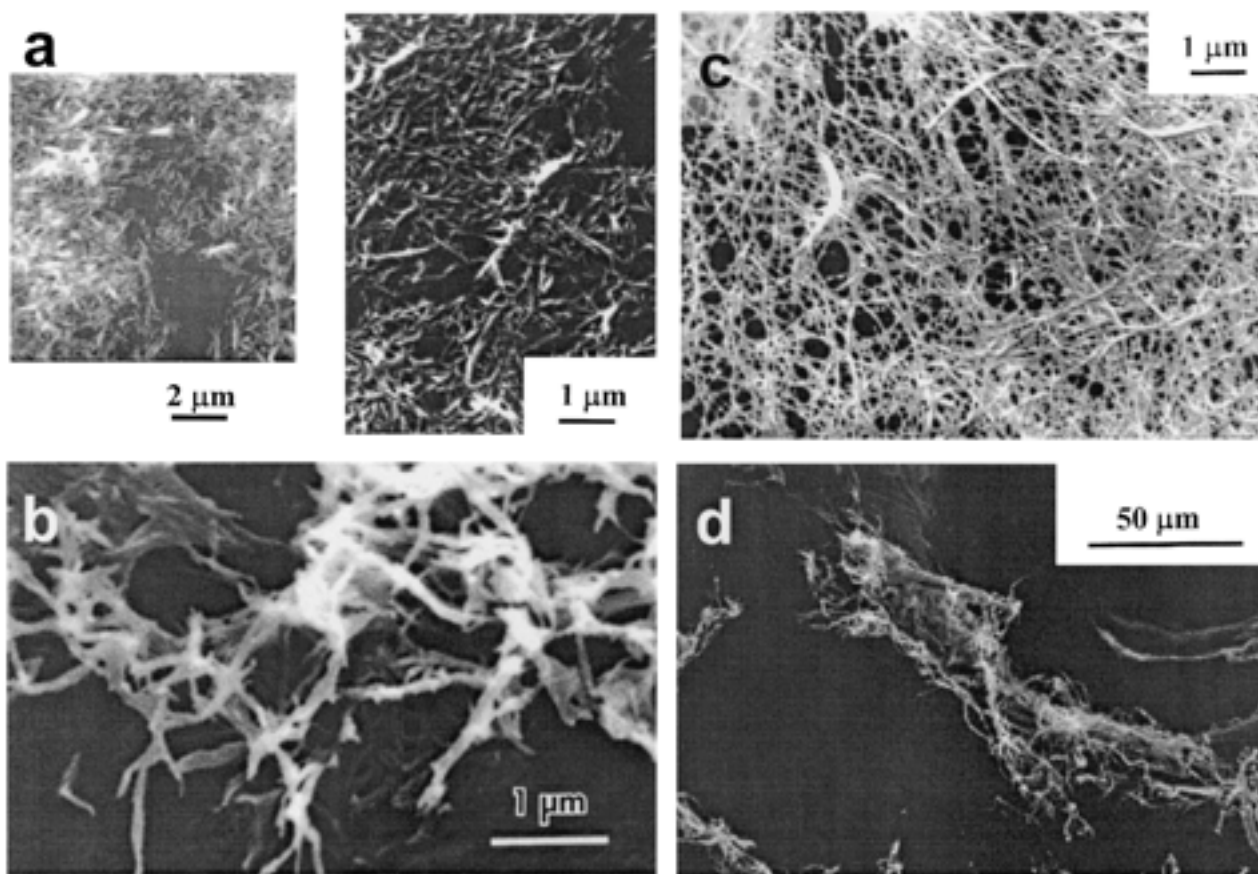


Fig.1 SEM Micrographs of cellulose fibers; a: Hydrolyzed CF11 (i.e., CF11H), the left side is an AFM image, b: Ceolus, c: Bacterial cellulose, d: Celish.

Table I The average sizes of cellulose fibers

Fiber	$L / \mu\text{m}$	$D / \mu\text{m}$	p
CF11H	0.72	0.017	42
Ceolus	1.7	0.077	22
BC	6–12	0.027	220–450
BCH	2.2	0.027	81
Celish	350	15	25

2.2 Measurements

The rheological properties were measured with a parallel-plates type rheometer (Rhosol-G2000, UBM Co., Ltd., Japan) devised to prevent vaporization of water. The diameters of the plates were 50 mm. All the measurements were performed at 30°C with varying fiber concentrations of the suspensions. The data were collected from low to high shear condition to avoid disrupting the suspension structure. The dynamic strain amplitude was 0.05, at which all the samples showed linear viscoelasticity. The fibers tend to aggregate gradually during the measurement, so that the measurements were carried out soon after the sample preparations.

3. RESULTS

3.1 Flow properties

The flow properties of the cellulose suspensions were examined by steady flow measurements. The gap between the plates of the rheometer should be sufficiently larger than the fiber length.¹¹⁾ We first examined the gap dependence of the measurements. Figure 2 shows logarithmic plots of the shear stress, σ , versus shear rate, $\dot{\gamma}$, for the Celish suspensions at a concentration of 0.3 wt%. When the gap was less than 1.0 mm, the flow curves depended on the gap and varied complicatedly. On the other hand, when the gap was 1.5 or 2.0 mm, the curve was smooth and the reproducibility was good. Therefore, a gap of 1.5 mm was selected for the following measurement of the Celish suspension. For the other fiber suspensions, there were no significant gap dependences. Even when the gap was as narrow as 0.5 mm, the measured flow curve was coincident with that measured using a cone-plate fixture. The gap was determined to be 1.0 mm for the measurement of the fiber suspensions except the Celish one.

Figure 3 shows the flow properties for the CF11H suspensions at various concentrations from 0 to 3.0 wt%. The 0 wt%, i.e., water, and the 0.1 wt% suspensions showed Newtonian flows. However, when the concentrations became higher than 0.3 wt%, the suspensions showed noticeably non-Newtonian flows. That is, the flow curves became flat for the abscissa. The values of the shear stress in the plateau region,

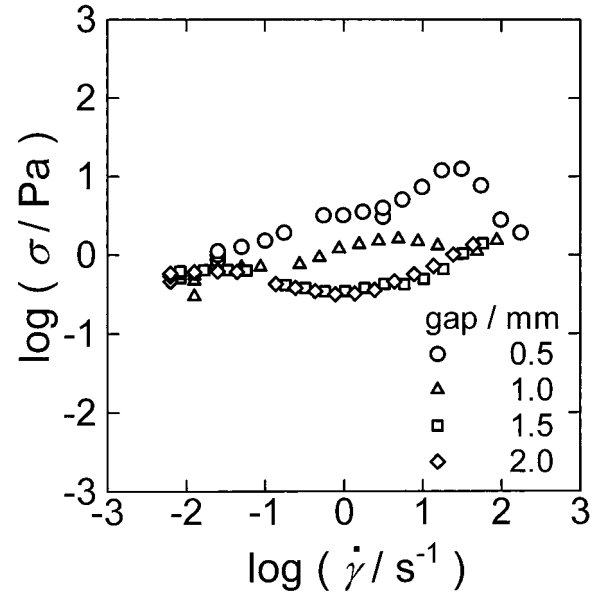


Fig.2 Effect of gap between plates on the flow curve of 0.3 wt% Celish suspension.

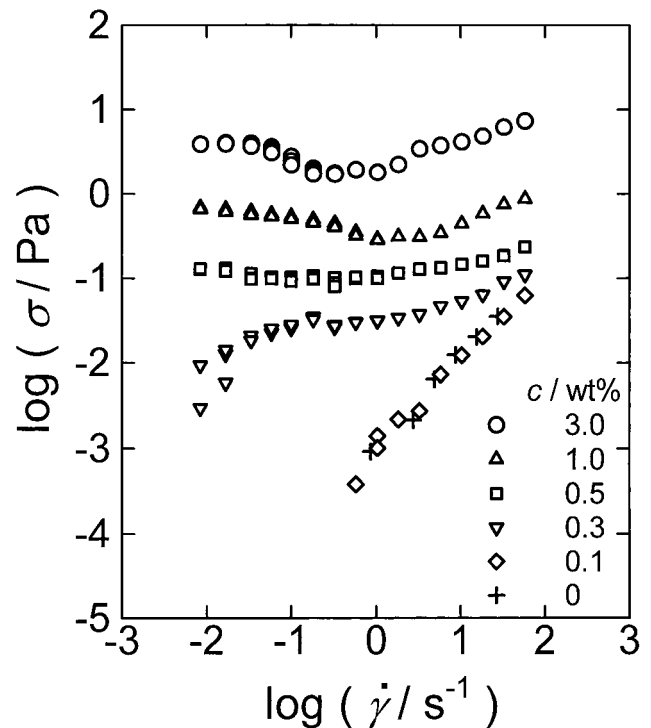


Fig.3 Logarithmic plots of shear stress, σ , versus shear rate, $\dot{\gamma}$, for various CF11H suspension concentrations, c .

which is designated as the yield stress, σ_y , of the suspension, increased with the fiber concentration. Figures 4 and 5 show the flow curves of the Celish and the BC suspensions. Although Celish is much larger than the other fibers, it does not sediment because of its microfibrillated surface. The flow curves of the Celish suspensions were very similar to those of the CF11H ones. On the contrary, the flow curves of the BC

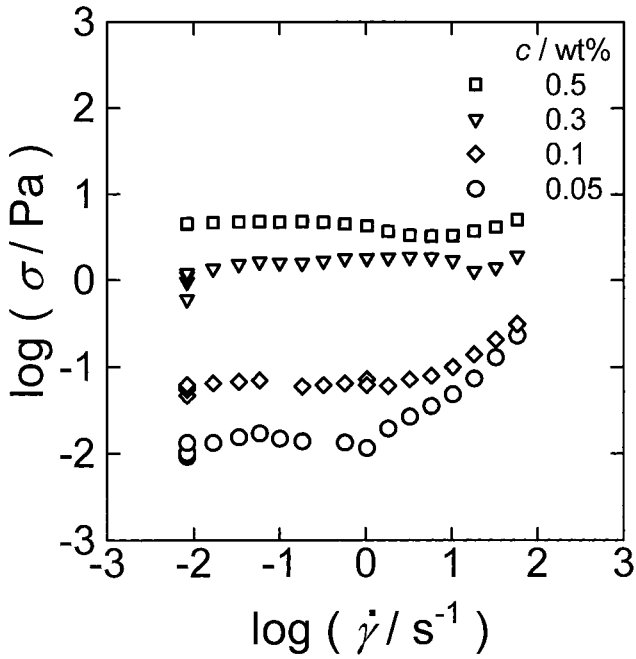


Fig.4 Logarithmic plots of shear stress, σ , versus shear rate, $\dot{\gamma}$, for various Celish suspension concentrations, c .

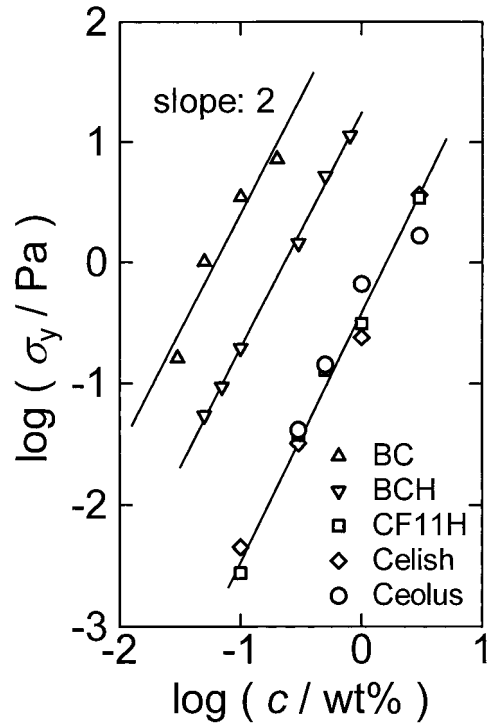


Fig.6 Logarithmic plots of yield stress, σ_y , versus fiber concentrations, c , for various fiber suspensions. $\dot{\gamma} = 0.01 \text{ s}^{-1}$.

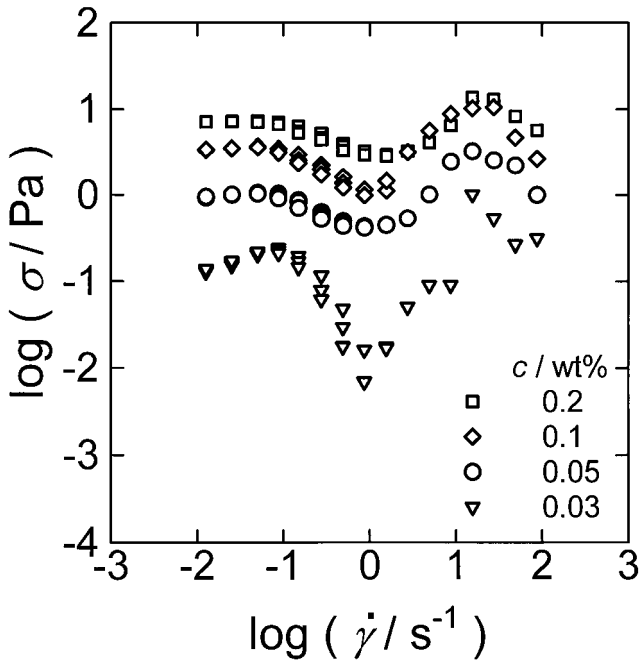


Fig.5 Logarithmic plots of shear stress, σ , versus shear rate, $\dot{\gamma}$, for various BC suspension concentrations, c .

suspensions were quite unique. There were stress drops in the middle $\dot{\gamma}$ region. The drops were noticeable at the low concentration. However, the tendency for the yield stress to increase with the fiber concentration was the same as that of the other fiber suspensions.

The yield stresses, σ_y , at $\dot{\gamma} = 0.01 \text{ s}^{-1}$ were logarithmically plotted versus the fiber concentrations, c , for all the suspensions and are shown in Fig.6. A power law relationship

with a power of 2 was fitted to the experimental data for all the suspensions. The BC suspension had the highest σ_y value in the measured sample at a certain concentration. The value became about one-tenth that of the original BC's due to the acid hydrolysis. The plots for CF11H, Celish, and Ceolus lay on a single line in spite of the variation in their size.

3.2 Dynamic viscoelasticity

The dynamic storage moduli, G' , and the loss moduli, G'' , plotted against the angular frequency, ω , for the CF11H suspensions are shown in Fig.7. The moduli were almost independent of ω at any fiber concentration. The G' values were about ten times that of G'' at the same concentration. They increased with the fiber concentration. The other fiber suspensions demonstrated almost the same rheological properties as the CF11H suspension. The plateau levels of the moduli, G' and G'' , at $\omega = 0.01 \text{ s}^{-1}$ were plotted against the fiber concentrations, c , for various cellulose suspensions as shown in Fig.8. The result is very similar to the plots of σ_y versus c shown in Fig.6. The moduli became smaller in the order, the BC, the BCH, and the other fiber suspensions, at a certain concentration. A single line was fitted to the data for the CF11H, the Celish, and the Ceolus suspensions. The moduli increased in proportion to $c^{9/4}$, regardless of the types of the fibers.

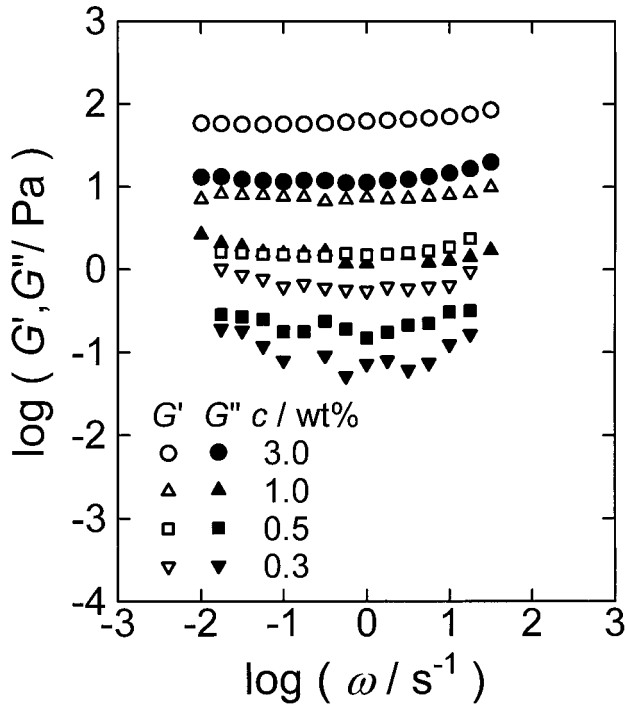


Fig.7 Logarithmic plots of dynamic storage moduli, G' , and dynamic loss moduli, G'' , versus angular frequency, ω , for various CF11H suspension concentrations, c .

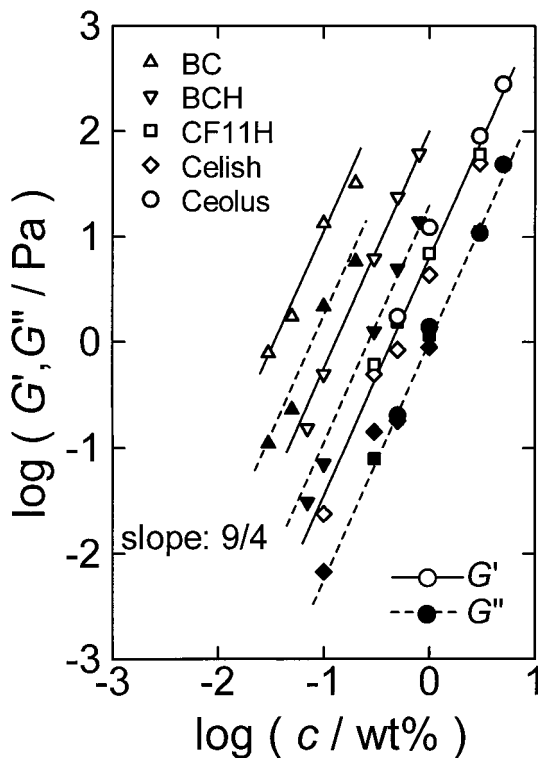


Fig.8 Logarithmic plots of dynamic moduli, G' and G'' , versus fiber concentrations, c , for various fiber suspensions. $\omega = 0.01 \text{ s}^{-1}$.

4. DISCUSSION

The concentration at which the flow behavior of a suspension shifts to a non-Newtonian from a Newtonian flow is considered as the critical concentration. The concentration of 0.3 wt% for the CF11H suspension was compared with c_0 calculated from Eq.(1). Using the axial ratio of the fiber listed in Table I, we obtained the critical concentration, c_0 , of 0.3 wt%. The calculated value agreed well with that evaluated by the rheological measurement. For the other microcrystalline cellulose suspensions (the Ceolus⁹) and the BCH suspensions), c_0 calculated from Eq.(1) also agreed well with the experimental results. The fact indicates that Mason's estimation¹⁾ can be applied to the microcrystalline cellulose fiber suspensions.

Fibers have a larger excluded volume than spherical particles. Therefore, the interaction between fibers is strong even at the low fiber suspension concentration. This is more remarkable as the fiber axial ratio becomes larger. In this case, the fibers tend to form flocs rather than remaining individual fibers because the former is more stable thermodynamically. The stress drops of the BC suspension in Fig.5 were thus considered to be derived from flocculation of the fibers. In practice, we observed the small flocs of the BC fibers after the steady flow measurement.

The plateaus of σ_y shown in Figs.3, 4, and 5 indicate that some network structures consisting of individual fibers were formed in the suspensions. The dynamic storage moduli of the suspensions also had plateaus as shown in Fig.7. It can be said that each suspension has a solid-like structure even at such low concentrations.

A power law relation was fitted to the data of σ_y versus c in Fig.6. The results almost agree with the earlier study.⁴⁾ This indicates that Eq.(2) can be applied over a wide range of fiber length and diameter. The power of 2 indicates that the origin of the yield stress is a two-body collision.

The other power law was also fitted to the dynamic data in Fig.8. The plots for the CF11H, the Celish, and the Ceolus suspensions lay on a single line. Their axial ratios, p , are almost the same, though their length and diameter differ from each other as shown in Table I. The moduli increased with p , so that the moduli are considered to be a function of p . Because the yield stress is related to G' , σ_y is also a function of p . Thus, the factor, k , in Eq.(2) is expressed by p , i.e., $k = k(p)$. Comparing Eq.(2) with Eq.(3), k is assumed to be in proportion to p^2 . By using the power relations between G' and c in Fig.8, the k values can be estimated, considering that G' is

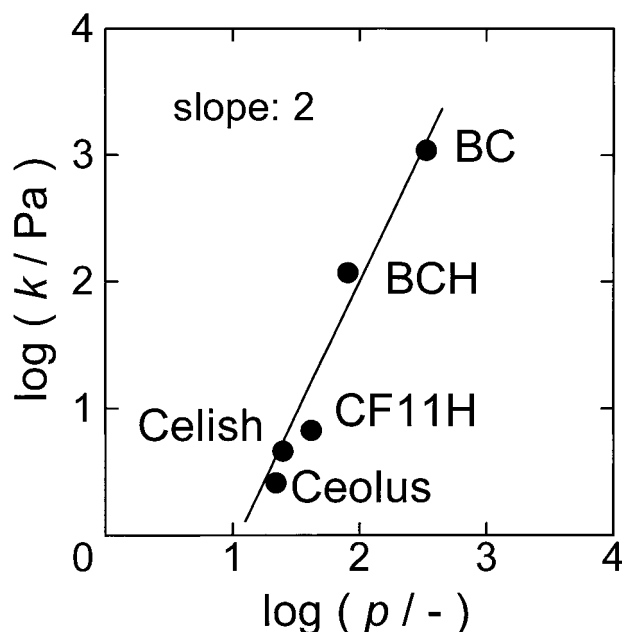


Fig.9 Logarithmic plots of the factor, k , versus axial ratio of fibers, p .

expressed as $G' = kc^\alpha$. The values for the BC, the BCH, the CF11H, the Celish, and the Ceolus suspensions are 1080, 120, 6.7, 4.6, and 2.6 Pa, respectively, when c is expressed by wt%.

The obtained k values were logarithmically plotted against the axial ratio, p , as shown in Fig.9. The result indicates that the k values are almost proportional to the square of the axial ratio of each fiber as we expected above. This fact suggests that k reflects individual fiber characteristics such as the axial ratio and Young's modulus of a fiber. On the contrary, the exponent value, α , did not change in spite of the variation in the fiber types as shown in Fig.8. This fact suggests that α does not reflect the individual characteristics of the fibers but the structural property of the whole suspension. The power agrees well with previous studies for that of pulp fiber suspensions.^{11,12} In addition, the power of 9/4 is consistent with that for polymer gels in a good solvent according to the scaling theory.¹³ This fact indicates that the rigidity of the fiber suspensions has appeared by the same mechanism from the order of cellulose fibers to microcrystalline cellulose fibers, even to polymer molecules.

5. CONCLUSIONS

The cellulose fiber suspensions show the yield stress, σ_y , and the pseudo-equilibrium modulus even at very low concentrations. A power law correlation was found between the moduli, G' , and the concentrations, c , of the suspensions, i.e., $G' = kc^\alpha$. The factor, k , changed with the types of the fibers, so that the k value reflects the individual fiber characteristics. On the other hand, the power, α , was constant around 9/4 over a wide range of fiber length and diameter, regardless of the types of fibers. This indicates that α reflects the structural property of the whole suspension.

REFERENCES

- 1) Mason SG, *Pulp Paper Mag Can* **51**, 94 (1950).
- 2) Forgacs OL, Robertson AA, Mason SG, "Fundamentals of Papermaking Fibres", Bolam F ed, (1958), Technical Section of the British Paper and Board Makers' Association, Kenley, p447.
- 3) Reeves DC, Gerischer GFR, *Appita* **35**, 316 (1982).
- 4) Kerekes RJ, Soszynski RM, Tam Doo PA, "Papermaking Raw Materials", Punton V ed, (1985), Mechanical Engineering Publications Limited, London, p265.
- 5) Bennington CPJ, Kerekes RJ, Grace JR, *Can J Chem Eng* **68**, 748 (1990).
- 6) Bennington CPJ, Kerekes RJ, Grace JR, *Can J Chem Eng* **69**, 251 (1991).
- 7) Bennington CPJ, Azevedo G, John DA, Birt SM, Wolgast BH, *J Pulp Paper Sci* **21**, J111 (1995).
- 8) Hietaniemi J, Gullichsen J, *J Pulp Paper Sci* **22**, J469 (1996).
- 9) Tatsumi D, Ishioka S, Matsumoto T, *Nihon Reorogi Gakkaishi* **27**, 243 (1999).
- 10) Araki J, Wada M, Kuga S, Okano T, *Colloid Surf A* **142**, 75 (1998).
- 11) Damani R, Powell RL, Hagen N, *Can J Chem Eng* **71**, 676 (1993).
- 12) Swerin A, Powell RL, Ödberg L, *Nord Pulp Paper Res J* **7**, 126 (1992).
- 13) de Gennes P-G, "Scaling Concepts in Polymer Physics", (1979), Cornell University Press, Ithaca.